JSME CENTENNIAL GRAND CONGRESS
International Conference on Fluid Engineering
Tokyo, Japan : July 13-16, 1997

JSME ICFE-97-716

A New Passive Device to Control Rotating Stall in Vaneless and Vaned Diffusers by Radial Grooves

Junichi Kurokawa, Jun Matsui, Takaya Kitahora and Sankar Lar Saha
Yokohama National University, Faculty of Engineering,
79-5 Tokiwadai, Hodogaya, Yokohama, 240 Japan

ABSTRACT

In order to control and suppress rotating stall in the diffuser of centrifugal turbomachine, a new passive device using radial shallow grooves is proposed and its effect is studied theoretically and experimentally. The results show that the radial grooves of 3 mm depth can suppress rotating stall in the vaneless and vaned diffusers over almost all flow ranges. The radial grooves of only 1 mm depth on both sidewalls can also suppress rotating stall.

Theoretical considerations have revealed that these remarkable effects of radial grooves are caused by two mechanisms; one is a significant decrease in tangential velocity due to the mixing between the main flow and the groove flow, and the other is an increase in radial velocity due to the reverse flow in the grooves.

INTRODUCTION

Rotating stall in vaneless and vaned diffusers not only make the stable operating range of pumps, fans and compressors very narrow, but also contribute severe damages to bearings[1]. As such, many studies have been performed so far[2]-[5] and the method has long been pursued to suppress this unstable phenomenon[6]. However, most of the methods so far proposed induce complicated mechanisms, and thus reduce overall efficiency of a turbomachine. Therefore, it is as yet a strong requirement to find a simple method of suppressing rotating stall.

One of the present authors has studied extensively on axial thrust, and has innovated that radial grooves have remarkable effect of reducing swirl strength of swirl flow[7]. Even though the radial grooves are very shallow with only 1 mm in depth, they can reduce the swirl strength remarkably. It is then predicted that such a device could be one possible way of controlling rotating stall in vaneless and vaned diffusers, as this unstable phenomenon occur in a relatively small discharge range with large tangential velocity.

The present study is thus aimed to reveal the effects of radial grooves mounted on the diffuser wall upon rotating stall in vaneless and vaned diffusers. In the first step of the study, the fundamental characteristics of rotating stall in a parallel-walled vaneless diffuser are determined experimentally. In the second step, the effect of radial grooves is shown upon suppressing rotating stall in vaneless and vaned diffusers experimentally. And finally, the mechanism of suppressing rotating stall using radial grooves is analyzed theoretically. The hydraulic loss caused by radial grooves is also determined experimentally.

EXPERIMENTAL APPARATUS AND PROCEDURES

In order to reveal the effect of radial grooves on suppressing rotating stall, two kinds of tests are conducted. One is the vaneless diffuser test and the other is the vaned diffuser test. Two kinds of parallel-walled diffuser test stands are shown in Figs.1 (a) and 1 (b). The dimensions and the notations of the impellers and the diffusers used in both tests are also shown in each figure. The impeller outlet width b_2 is equal to the diffuser width b. In each test stand a variable speed motor is set to control the speed of the centrifugal impeller, and a supplemental blower is set at the upstream to control the flow rate widely.

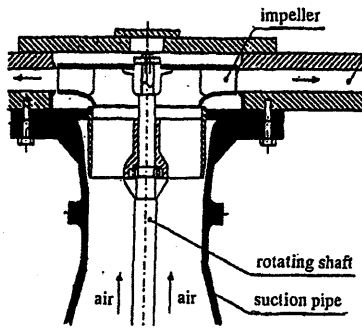

(a) Vaneless Diffuser test stand

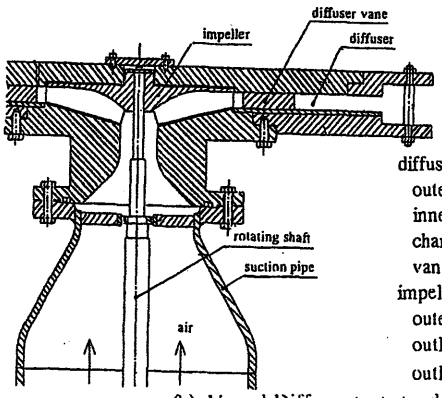

(b) Vaned Diffuser test stand

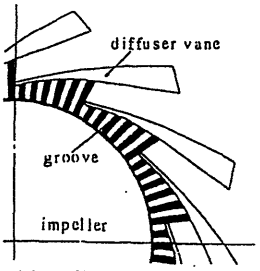

(c) Diffuser vanes and radial grooves

Fig. 1 Test stand

The configuration of a diffuser vane in the vaned diffuser test is illustrated in Fig. 1 (c), where the vanes are set at the radius ratio of $R = r/r_i = 1.10$ and the vane angle $\beta_v = 9°$. When β_v was larger than 16°, no rotating stall occurred in all flow ranges.

The radial grooves used in the vaneless diffuser tests are of the width w=10 *mm*, the depth d=1 or 3 *mm* and the number of grooves n is varied from 4 to 32. The groove length is equal to $(r_o - r_i)$ and short grooves of 50, 70 and 125 *mm* in length are also tested. In the vaned diffuser test 78 grooves of w=5 *mm* and d=3 *mm* are used. In both of the tests the impeller speed is 3000 *rpm*, and the corresponding Reynolds number $Re \equiv u_2 r_2/\nu$ is 3.3×10^5, where u_2 is the impeller tip speed and ν is the kinematic viscosity of working fluid.

EXPERIMENTAL RESULTS AND DISCUSSIONS

Characteristics of Rotating Stall in a Vaneless Diffuser

The wall pressure fluctuations measured at the radius ratio of $R \equiv r/r_2 = 1.10$ in the vaneless diffuser are plotted in Fig. 2. The flow angle α is defined as $\alpha \equiv \tan^{-1}(\overline{v_r}/\overline{v_\theta})$, where $\overline{v_r}$ and $\overline{v_\theta}$ are the sectional-averaged radial and tangential velocity components.

When the flow angle is decreased by throttling the inlet flow, a periodical pressure fluctuation initiates at the flow angle α of about 26°, corresponding to the flow coefficient of $\phi \equiv Q/2\pi r_2 b_2 u_2 = 0.33$, where Q is the flow rate. This fluctuation grows to a clear sinusoidal oscillation as shown in Fig. 2(a). The pressure data measured at three different points in the tangential direction revealed that this oscillation is due to the rotating stall with two cells. With further decrease in flow rate, both the frequency and the amplitude increase as shown in Figs. 2(b) and (c), and the oscillation changes from a sinusoidal wave to a triangular wave superimposed with higher harmonic waves. The amplitude of two-cell-oscillation takes the maximum value near the flow angle of α=15° and decreases with further decrease in α. Around α= 12°, another oscillation with much lower frequency is imposed to two-cell-oscillation as shown in Figs. 2(d) and (e). The phase measurement has revealed that this oscillation is the rotating stall with one cell.

With further decrease in the flow rate, the one-cell-oscillation becomes prominent as shown in Figs. 2 (e) and (f), and grows to a large pressure fluctuation whose amplitude amounts to about twice that of two-cell-oscillation. The frequency of this oscillation increases with a decrease in the flow angle until α=5° and then decreases as shown in Fig. 2 (g), while the amplitude of two-cell-oscillation decreases monotonously and disappears. In the range of α< 2° the rotating stall disappears as shown in Fig. 2 (h).

The behavior of the present rotating stall described above seems to be much different from that previously reported[1]-[6]. To show the difference more clearly the non-dimensional amplitude and frequency are calculated and are shown in Figs. 3 (a) and (b). Here, the non-dimensional frequency Ω is defined as[2]

$$\Omega \equiv 2\pi r_o^2 f / (v_{0i} r_i m) \qquad (1)$$

where, f and m are the frequency and the number of cells respectively, and v_{0i} is the tangential velocity at the diffuser inlet.

Figure 3(a) reveals that the largest pressure fluctuation occurs when both one-cell-stall and two-cell-stall coexist and its range is 5°< α <13° in the case of 3000 rpm.

According to the results[3]-[5], the non-dimensional frequency Ω shows slight change or no change with α and takes the value of Ω =1.1~1.2. But Fig. 3 (b) shows that Ω changes largely with α. Ω is rewritten as $\Omega = (2\pi r_o f/m)/(v_{0i} r_i/r_o)$, in which the numerator

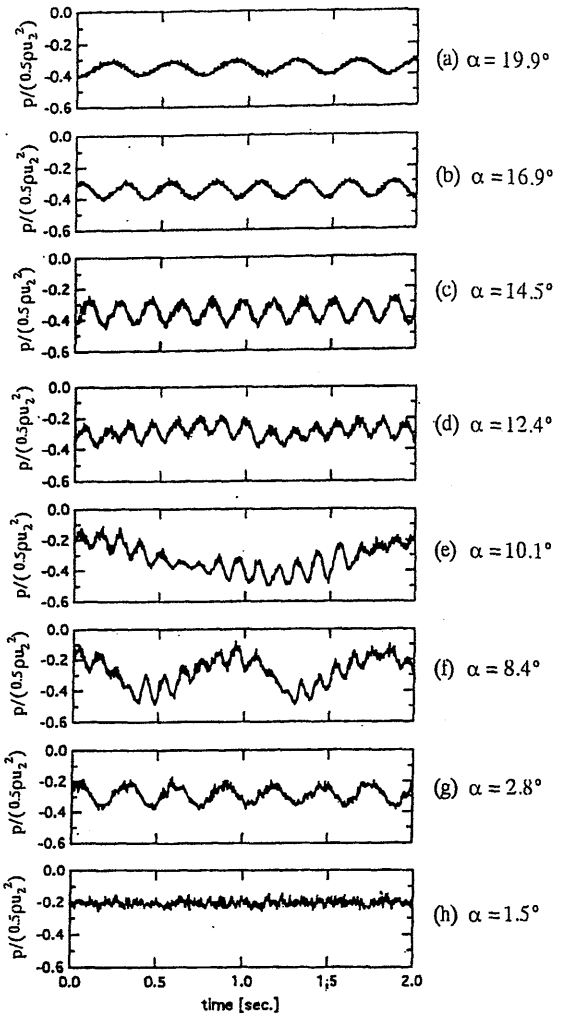

Fig. 2 Pressure fluctuation measured at R=1.10 in vaneless diffuser

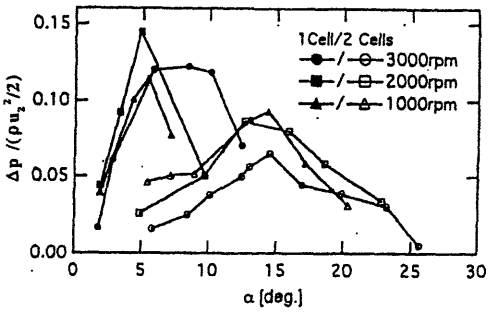

(a) Non-dimensional amplitude

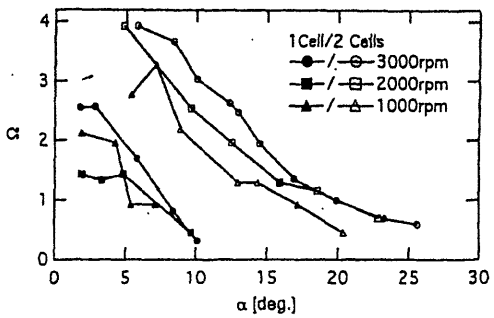

(b) Non-dimensional frequency

Fig. 3 Characteristics of wall pressure fluctuation of rotating stall in vaneless diffuser with large radius ratio: r_o/r_i=4.78

$2\pi r_o f/m$ is the stall propagation velocity per one cell at the diffuser outlet and the denominator $v_{0i}\, r_i/r_o$ is the fluid tangential velocity at the diffuser outlet. The constant Ω value of the results[3]-[5] then shows that the stall propagation velocity mainly depends upon the outlet flow characteristics of the diffuser.

On the contrary, the present results show that the stall propagation velocity is largely influenced by the flow angle α, i. e., by the flow behavior inside the diffuser rather than the flow behavior at the diffuser outlet. Further investigation has revealed that almost all of the diffusers used in the conventional studies had much smaller radius ratio of $r_o/r_i<2.0$, than that of the present diffuser $r_o/r_i=4.78$. According to Jansen[2] and Tsujimoto[3], the reverse flow near the wall could be the cause of rotating stall. In a small-sized diffuser, this reverse flow region soon expands to the diffuser outlet with a decrease of α and after that the rotating stall should show similar behavior against a decrease of α, while in a large-sized diffuser the reverse flow region near the wall hardly expands to the diffuser outlet and the rotating stall should show several different patterns with a decrease of α. Thus, it is concluded that the present diffuser may give more general behavior of rotating stall than the conventional ones.

Suppression of Rotating Stall in a Vaneless Diffuser by Radial Grooves

In order to suppress rotating stall in a vaneless diffuser, several kinds of radial grooves were tested. Radial grooves were mounted on one sidewall or both sidewalls, and the effect of grooves was revealed experimentally together with the hydraulic loss caused by the radial grooves.

In the first step of the measurements, the number n of the grooves was increased for the fixed depth of d=3 mm and the width of w=10 mm. With an increase in number of grooves from 4, the amplitude of wall pressure fluctuation decreased remarkably and the flow rate range of rotating stall also decreased largely. But it was not until n=32, when the stall was completely suppressed over the whole flow range. As an example, the wall pressure fluctuation measured at R=1.10 is compared with the no-grooved case in Fig. 4. This is the case of the largest pressure fluctuation, that is, at $\alpha \approx 8.4°$. Referring to Fig. 2 (f), it is clearly seen that the periodic pressure fluctuation is completely suppressed.

Several kinds of grooves with various dimensions were further tested and it was revealed that the groove dimensions which could suppress the rotating stall completely in all flow ranges were $32^n \times 3\ \mathrm{mm}^d \times 10\ \mathrm{mm}^w$ on one sidewall and $32^n \times 1\ \mathrm{mm}^d \times 10\ \mathrm{mm}^w$ on both sidewalls. The larger dimensions than those mentioned here can suppress rotating stall completely for all flow ranges.

The sectional velocity profiles at R=1.10 in these cases are compared in Figs. 5 (a) and (b), in which z is the distance from the upper wall. Figure 5 (a) shows that the decrease in tangential velocity v_θ caused by shallow grooves is surprisingly large, though the change of radial velocity v_r is limited only near the wall as shown in Fig. 5 (b).

The short grooves were also tested and the results showed that they could also suppress rotating stall remarkably. For example, the grooves of 50 mm in length and of $32^n \times 3^d \times 10^w$ on one sidewall reduces the range of rotating stall from $\alpha \leq 26°$ to $\alpha \leq 7°$ and the amplitude to a half. Although they could not suppress rotating stall completely, yet they were very effective.

The use of radial grooves is inevitably associated with the reduction of the overall performance of a turbomachine, because they decrease the tangential velocity of the diffuser flow. However, the reduction of tangential velocity also decreases the friction loss in diffuser, which improves the diffuser performance. In order to

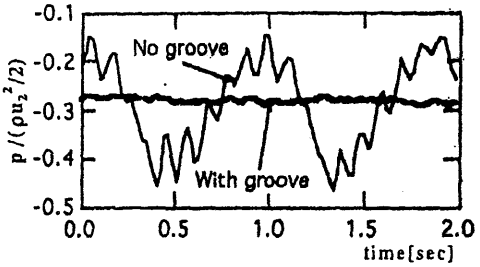

Fig. 4 Effect of radial grooves on suppressing rotating stall in vaneless diffuser (grooves: $32^n \times 3^d \times 10^w$)

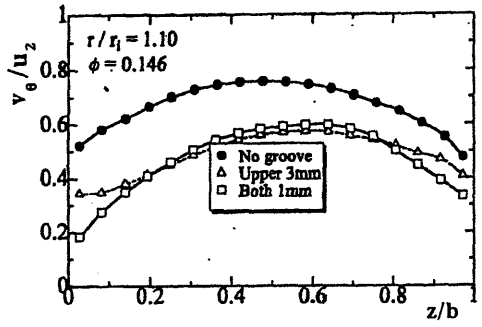

(a) Tangential velocity

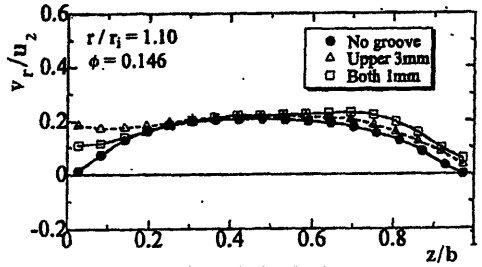

(b) Radial velocity

Fig. 5 Velocity distribution measured at R=1.10 (ϕ=0.146)

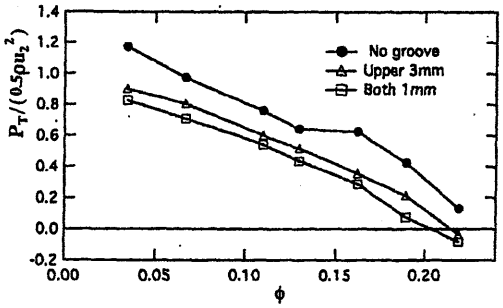

(a) R=1.10 (impeller outlet)

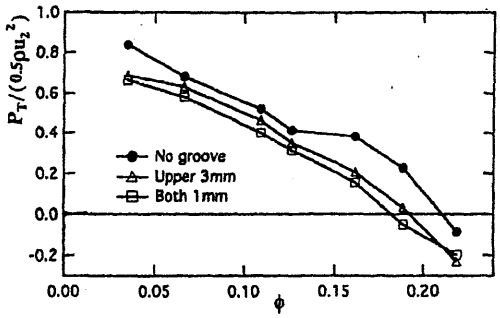

(b) R=4.78 (diffuser outlet)

Fig. 6 Total pressure in the vaneless diffuser

examine the total hydraulic loss increase, the total pressures are measured at the upstream and the outlet of the impeller, R=1.10. The total pressure at the diffuser outlet is the atmospheric pressure.

The total pressure differences at R=1.10 and at the diffuser outlet from the impeller inlet are plotted in Figs. 6 (a) and 6 (b) respectively and only for the case of the most effective groove dimensions. Comparison of Fig. 6 (a) with 6 (b) reveals that the hydraulic loss amounts to about $0.2\times\rho u_2^2/2$ at the impeller outlet (Fig. 6 (a)), but about $0.1\times\rho u_2^2/2$ is recovered in the diffuser channel (Fig. 6 (b)). This means that the increase in total loss by grooves is about 10% of $\rho u_2^2/2$. Here, it is to be noted that in the largest pressure fluctuating range around ϕ~0.12, the total pressure loss takes the minimum value of about 5% of $\rho u_2^2/2$.

As the total pressure at the impeller outlet depends mainly upon the impeller specific speed, it is difficult to deduce a general conclusion. However, it should be remarked that the total pressure loss of $0.05\times\rho u_2^2/2$ is the compensation for the suppression of the most severe pressure fluctuation.

Suppression of Rotating Stall in a Vaned Diffuser

With a decrease in flow rate in the vaned diffuser test, rotating stall initiated at the flow rate around ϕ=0.020, and the pressure fluctuation showed a triangular wave, which is typical for the rotating stall of a vaned diffuser. With further decrease in flow rate the amplitude of the pressure fluctuation showed no change and the frequency increased a little. Figure 7(a) illustrates the typical fluctuation measured at R=1.10 and at the middle of the vaned channel for the case of ϕ=0.014.

In order to suppress the rotating stall, the radial grooves of n=78, d=3 mm and w=5 mm are used on both sidewalls as shown in Fig. 1 (c). Since the area between the impeller outlet and the diffuser vane inlet is very small, the number of the grooves is increased much more than the vaneless diffuser case. The effect of grooves is illustrated in Fig. 7 (b). The rotating stall is shown to be suppressed and no periodical pressure fluctuation is seen.

When the grooved wall is used, an increase of hydraulic loss is inevitably associated. The total pressure variations are compared in Fig.8 among the no groove case □, the grooved-wall case △ and the vaneless diffuser case ●. In the vaneless diffuser case rotating stall occurred in all flow ranges and the total pressure is the smallest among the three(□, △, ●) over the whole flow range. In the vaned diffuser case with no groove the total pressure suddenly drops due to the initiation of rotating stall around ϕ=0.020. In the vaned diffuser with grooves, the total pressure takes the intermediate values between the vaned diffuser and the vaneless diffuser over the whole flow range, and the hydraulic loss due to the grooves amounts to about 8% of $\rho u_2^2/2$. In this case the rotating stall was completely suppressed over all flow ranges but for a very low range of ϕ<0.005, the total pressure dropped as shown in Fig. 8.

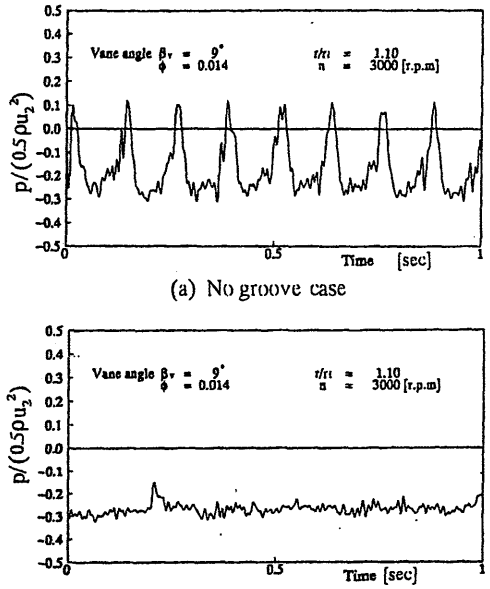

(a) No groove case

(b) Grooved case (grooves: $78^n\times3^d\times5^w$ on both sidewalls)

Fig. 7 Effect of grooves on pressure fluctuation of rotating stall in vaned diffuser

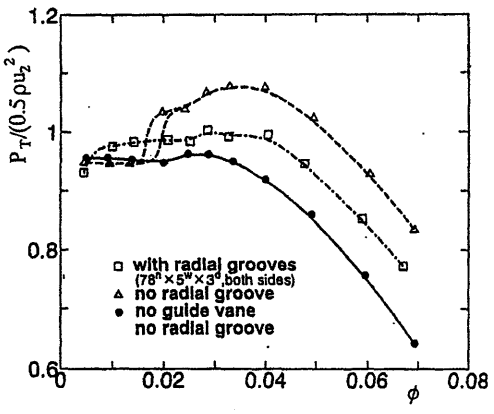

Fig. 8 Total pressure difference between impeller inlet and vaned diffuser outlet

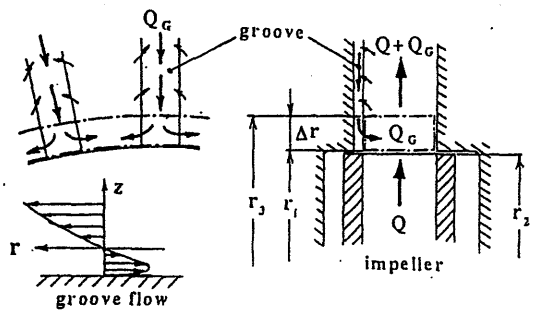

Fig. 9 Flow near the inlet of vaneless diffuser with radial grooves

MECHANISM OF SUPPRESSING ROTATING STALL BY RADIAL GROOVES

Theoretical Consideration

In order to elucidate the mechanism of suppressing rotating stall, the effects of radial grooves are studied theoretically. The purpose of the analysis is to reveal the change of mean flow characteristics by providing radial grooves, and thus the steady incompressible flow in a parallel-walled vaneless diffuser with grooves is analyzed in the followings.

Rotating stall generally occurs in the low flow range where the radial velocity v_r is much smaller than the tangential velocity v_θ. Supposing $v_r \ll v_\theta$ in the vaneless diffuser with radial grooves, the equations of angular momentum balance, momentum balance and of continuity are written as follows using the notations in Fig. 9:

$$d/dr[2\pi\rho r^2 b\overline{v_r v_\theta}] - \rho r\overline{v_\theta}(dQ_G/dr) = -4\pi r^2\tau_0 \qquad (2)$$

$$dp/dr = \rho\overline{v_\theta}^2/r \tag{3}$$

$$2\pi r b\overline{v_r} = Q \tag{4}$$

where, bar denotes the averaged value over the section from the upper wall z=0 to the lower wall z=b, and the double bar denotes the mass-averaged one. Q_G is the flow rate of the groove flow. In the momentum equation (3), the integration $\int v_\theta^2 dz$ is approximated to $(\int v_\theta dz)^2$, and the error due to this approximation amounts up to 2% at most. The second term in the left hand of Eq. (2) represents the loss of angular momentum caused by the flow coming into the groove. If the groove flow comes into the main flow, this term should be considered as 0.

The tangential component of the shearing stress τ_θ in Eq. (2) is expressed as follows when the flow distortion parameter $K'(\equiv \overline{\overline{v}_\theta}/v_{\theta max})$ is introduced[8].

$$\tau_\theta = C_f\rho\, v_{max} v_{\theta max}/2 = C_f\rho(\overline{\overline{v}_\theta}/K')^2/2\cos\alpha$$
$$C_f = 0.049(\nu K' \sin\alpha/\tau v_\theta)^{0.184}/(\cos\alpha)^{0.816} \tag{5}$$

The flow distortion parameter K' is expressed as follows[8] for the case of b_2=b:

$$K' \equiv \overline{\overline{v}_\theta}/v_{\theta max} = 0.88K,\quad K \equiv \overline{\overline{v}_\theta}/\overline{v_\theta} = 0.812/\phi^{0.114} \tag{6}$$

Generally speaking, the groove flow is driven by the radial pressure gradient and thus flows in the inward direction. The balance of forces in the groove is then expressed as

$$A\,dp = \tau_0 s\,dr,\quad \tau_0 = 0.108\rho(Q_G/A)^2(\nu A//Q_G d)^{0.25} \tag{7}$$

where, A and s are the sectional area and the wetted surface length of the groove, respectively. τ_0 is the wall shearing stress on the groove wall and is expressed as shown above referring to Blasius.

Introducing Eqs. (3)~(7) into Eq. (2) yields the following non-dimensional equation.

$$\{\phi + a(V_\theta^2/R)^{4/7}\}R dV_\theta/dR = -V_\theta\{\phi + a(V_\theta^2/R)^{4/7}\} - b(\sin\alpha)^{0.184}(RV_\theta/\cos\alpha)^{1.816} \tag{8}$$

where, $V_\theta \equiv \overline{\overline{v}_\theta}/u_2$ and $R \equiv r/r_2$. a and b are expressed as

$$a = 0.568\,Re^{1/7}(D^{12/7}W^{11/7}n)/(D+W)^{4/7}B_2K^{8/7}$$
$$b = 0.049/Re^{0.184}K'^{0.186}B_2$$

where, $D \equiv d/r_2$, $W \equiv w/r_2$ and $B_2 \equiv b_2/r_2$.

If there is no groove, a becomes 0 and Eq. (8) can be solved analytically to give ;

$$V_\theta = \frac{V_{\theta 2}}{R}\left\{1 + \frac{0.0400(\sin\alpha_2/\mathrm{Re})^{0.184}V_{\theta 2}^{0.186}(R-1)}{\phi B_2(K'\cos\alpha_2)^{1.816}}\right\} \tag{9}$$

The effects of grooves are to be determined from Eq. (8) numerically, which requires the boundary value $V_{\theta 2}$ at R=1.0. The boundary value $V_{\theta 2}$ is predicted from Eq. (9) by giving the following empirical relation measured at R=1.10 in the no groove case.

$$\alpha_3 = 78.3\phi \quad (\text{at R=1.10}) \tag{10}$$

When the grooves are mounted on the diffuser wall, the groove flow comes inward in the groove and mixes with the main flow resulting in a sudden drop of the boundary value at R=1.0.

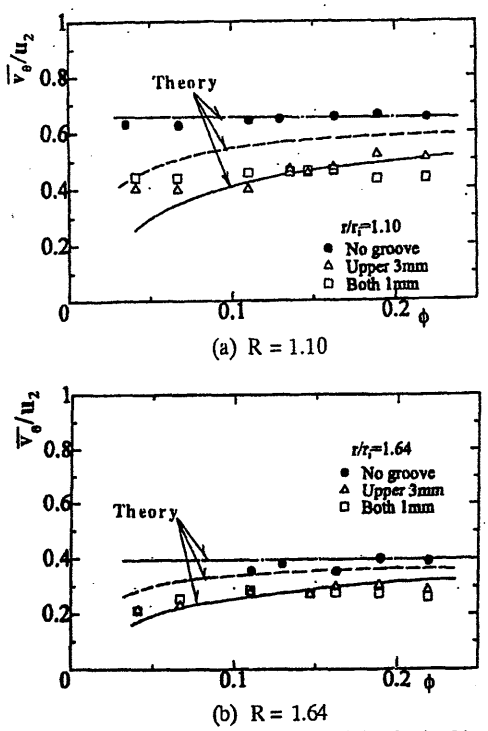

(a) R = 1.10

(b) R = 1.64

Fig. 10 Comparison of predicted tangential velocity V_θ with measurements for the variation of discharge coefficient ϕ

Here it is supposed that the main flow and the groove flow soon mix to be uniform in the small region Δr shown in Fig. 9. The angular momentum balance in this small control volume determines the value $V_{\theta 3}(\equiv \overline{\overline{v}_{\theta 3}}/u_2)$ at $R=1+\Delta r/r_2$, and is expressed as

$$\rho r_2\overline{\overline{v}_{\theta 2}}Q = \rho r_3\overline{\overline{v}_{\theta 3}}(Q + Q_{G2}) + 2\int 2\pi r^2\tau_\theta dr \tag{11}$$

Comparison and Discussions of Theoretical Data and Vaneless Diffuser Test Data

The conspicuous effect of radial grooves is to decrease the tangential velocity of the main flow as is already shown in Fig. 5(a). To confirm the validity of the theory, comparison of the theoretical and measured tangential velocity $\overline{v_\theta}$ is shown in Fig. 10(a) at R=1.10 and Fig. 10(b) at R=1.64. Three cases are plotted, the no groove case (●), the grooved wall case of 1 mm depth on both walls (□) and that of 3 mm depth on the upper wall (△).

Figure 10(a) reveals that $\overline{v_\theta}$ near the diffuser inlet decreases remarkably over the whole flow range by the grooves of only 1 mm depth, and that the groove effect increases with a decrease in ϕ. But the decrease of $\overline{v_\theta}$ is relatively small at R=1.64 from Fig. 10(b). The present theory is seen to give good prediction to the measured data of 3 mm depth case. Here it is to be remarked that the 1 mm-depth-groove on both walls has almost the same effect as the 3 mm-depth-groove on one sidewall, though the theory does not well agree with the 1mm-depth-groove. This might be due to a rapid increase of radial velocity near the wall which is not considered in the theory based on the mean flow.

To discuss the mechanism of suppressing rotating stall by shallow grooves, the change of flow angle α is illustrated in Figs. 11 (a) at R=1.10 and 11 (b) at R=1.64. A considerable uniform increase of α is caused for over all discharge ranges, and this increase is seen not locally but over the whole diffuser region. It is

also revealed that complete suppression of rotating stall for over all flow ranges requires about 7.5~8.5° increase of the mean flow angle at R=1.10. If the increase of α were caused only by the decrease of tangential velocity, it would become much smaller than that shown in Fig. 11. This means that the radial velocity v_r also increases largely. To show this more clearly, the theoretical results of the flow rate ratio Q_G/Q at R=1.10 are illustrated in Fig. 12. It is surprising that the flow rate amounts to more than 40% of the main flow in the shallow grooves of 3 mm depth in the low flow range. As the increase of v_r is limited to the vicinity of the wall as shown in Fig. 5(b), the flow angle near the wall should become much larger.

To reveal the detailed mechanism of suppressing rotating stall by the grooves, the contribution of mixing between the main flow and the groove flow is separated in the theory by neglecting Eq. (11). The increase of α then becomes 3.5~4° for all flow ranges at R=1.10 in the case of 3 mm-depth-groove, which is half of the total increase of α.

Accordingly, it is concluded that remarkable effects of radial grooves are caused by the following two mechanisms; one is a remarkable decrease of tangential velocity at the diffuser inlet due to the mixing between the main flow and the groove flow, and the other is a remarkable increase of radial velocity due to the reverse flow in the grooves. Both the effects have the same weight of contribution to increase the flow angle. Even if the groove is very shallow such as d=1 mm, the increase of flow angle is very large near the wall, which suppresses rotating stall over the whole flow range.

CONCLUSIONS

In order to suppress rotating stall in vaneless and vaned diffusers, a new passive device using radial grooves is proposed and its effect is confirmed theoretically and experimentally, and the characteristics of rotating stall in a large-sized diffuser are determined. The conclusions are summarized as follows;

(1) Though the shallow radial grooves are very simple, the effect of decreasing flow angle is conspicuous. Using the groove dimensions of $32^n \times 3^d \times 10^w$ on one sidewall or $32^n \times 1^d \times 10^w$ on both walls, the rotating stall in a vaneless diffuser is completely suppressed in all flow ranges. Using the short grooves of $78^n \times 3^d \times 5^w$, the rotating stall in a vaned diffuser is also completely suppressed in almost all flow ranges.

(2) The theory has revealed the mechanism of suppressing rotating stall by radial grooves, i. e., the following two mechanisms; one is a remarkable decrease of tangential velocity at the diffuser inlet due to the mixing between the main flow and the groove flow, and the other is the remarkable increase of radial velocity due to the reverse flow in the grooves. Both effects have the same weight of contribution to increase the flow angle. Since the increase of a flow angle is especially large near the wall, the shallow grooves on both the walls have nearly the same effect as the deeper grooves on one side wall.

(3) To suppress the largest pressure fluctuation of rotating stall requires 7.5~8.5° increase of a flow angle. But the radial grooves reduce the flow angle uniformly in all flow ranges. This causes additional hydraulic loss of (5~10)%of $\rho u_2^2/2$ in a vaneless diffuser and about 8% of $\rho u_2^2/2$ in a vaned diffuser.

(4) Rotating stall in a large-sized vaneless diffuser shows many different patterns depending on the flow angle, as the region of the reverse flow induced near the wall hardly expands to the diffuser outlet. On the contrary, in a small-sized diffuser the flow pattern of rotating stall changes little with the change of a flow angle.

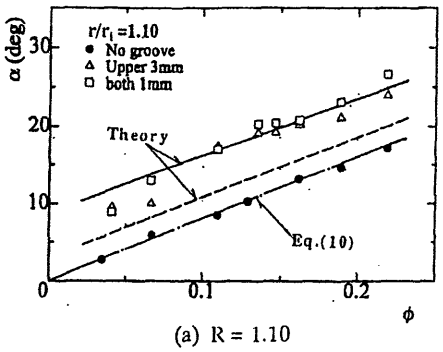

(a) R = 1.10

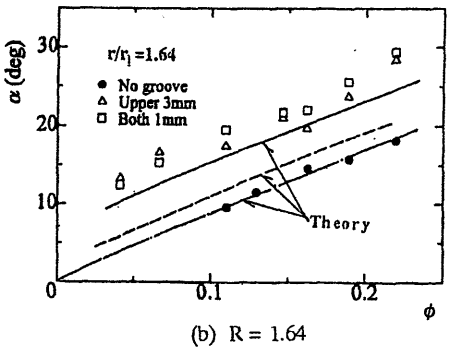

(b) R = 1.64

Fig. 11 Comparison of flow angle between theory and measurements

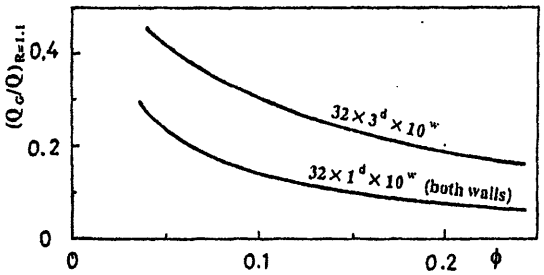

Fig. 12 Flow rate ratio of main flow and groove flow at R=1.10

REFERENCES

(1) Greitzer, E.M., The Stability of Pumping System, *Trans. ASME*, Ser. I, Vol. 103 (1981), p.193

(2) Jansen, W., Rotating Stall in a Radial Vaneless Diffuser, *Trans. ASME, Jr. Basic Engineering*, Vol. 86, No. 4(1964), pp. 750-758.

(3) Senoo, Y. and Kinoshita, Y., Limits of Rotating Stall in Vaneless Diffuser of Centrifugal Compressors, *ASME Paper* No. 78-GT-19(Apr. 1978).

(4) Tsurusaki, H.,Effects of Diffuser Geometry on RotatingStall in Vaneless Diffuser, *Trans. JSME (in Japanese)*, Vol. 59, No. 566(1993), pp. 3133-3139.

(5) Watanabe, H. and Ariga, I., Transient Process of Rotating Stall in Radial Vaneless Diffuser, *Trans. JSME (in Japanese)*, Vol. 59, No. 565(1993), pp. 2848-2853.

(6) Yosida, Y. Murakami, Y., Tsurusaki, H. and Tsujimoto Y. Rotating Stall in Centrifugal Impeller/Vaned Diffuser Systems, Proc. ASME-JSME Joint Conf. (Portland), FED-Vol.107(1991).

(7) Kurokawa, J., Kamijo, K. and Shimura, T., Axial Thrust Behavior in LOX-Pump of Rocket Engine, *AIAA, Jr. Propulsion and Power*, Vol. 10 No. 2(1994), pp. 244-250.(9)

(8) Kurokawa, J. and Hode S., Prediction of Outlet Flow Characteristics of Centrifugal Impellers(1st Rep.), *Bulletin JSME*, Vol.28,No.241(1985), pp. 1423-1429.